

Calculating the energy required to undergo the conditioning phase of a titanium alloy inertia friction weld

Turner, Richard; Howe, Daniel; Ward, Mark; Thota, Bhaskar ; Basoalto, Hector; Brooks, Jeffery

DOI:

[10.1016/j.jmapro.2016.09.008](https://doi.org/10.1016/j.jmapro.2016.09.008)

License:

Creative Commons: Attribution-NonCommercial-NoDerivs (CC BY-NC-ND)

Document Version

Peer reviewed version

Citation for published version (Harvard):

Turner, R, Howe, D, Ward, M, Thota, B, Basoalto, H & Brooks, J 2016, 'Calculating the energy required to undergo the conditioning phase of a titanium alloy inertia friction weld', *Journal of Manufacturing Processes*, vol. 24, no. 1, pp. 186–194. <https://doi.org/10.1016/j.jmapro.2016.09.008>

[Link to publication on Research at Birmingham portal](#)

Publisher Rights Statement:

Validated 10/10/2016

General rights

Unless a licence is specified above, all rights (including copyright and moral rights) in this document are retained by the authors and/or the copyright holders. The express permission of the copyright holder must be obtained for any use of this material other than for purposes permitted by law.

- Users may freely distribute the URL that is used to identify this publication.
- Users may download and/or print one copy of the publication from the University of Birmingham research portal for the purpose of private study or non-commercial research.
- User may use extracts from the document in line with the concept of 'fair dealing' under the Copyright, Designs and Patents Act 1988 (?)
- Users may not further distribute the material nor use it for the purposes of commercial gain.

Where a licence is displayed above, please note the terms and conditions of the licence govern your use of this document.

When citing, please reference the published version.

Take down policy

While the University of Birmingham exercises care and attention in making items available there are rare occasions when an item has been uploaded in error or has been deemed to be commercially or otherwise sensitive.

If you believe that this is the case for this document, please contact UBIRA@lists.bham.ac.uk providing details and we will remove access to the work immediately and investigate.

Calculating the energy required to undergo the conditioning phase of a titanium alloy inertia friction weld

R.P. Turner^{a*}, D. Howe^b, B. Thota^a, R.M. Ward^a, H.C. Basoalto^a and J.W. Brooks^a

^a PRISM² Research Group, Metallurgy & Materials, University of Birmingham, Birmingham, B15 2TT, UK.

^b Rolls-Royce plc, Materials & Process Modelling, PO Box 31, Derby DE24 8BJ.

* Contact email address for corresponding author: r.p.turner@bham.ac.uk

Abstract

Inertia friction welding (IFW), a type of rotary friction welding process, is widely used across aerospace, automotive and power-generation industries. The process considers a specialist rotary friction welding machine, which asks for the critical process parameters of Inertial mass, initial rotational speed and applied pressure, to complete the relevant weld. The total kinetic energy available to the system can be calculated from basic physical relationships for the kinetic energy stored in a flywheel. This kinetic energy must be converted partly to heating the specimen at the interface, and partly to mechanical work via deformations. A finite element (FE) numerical model has been developed to predict the steady-state thermal profiles formed at the onset of mechanical deformation. Therefore, the amount of this total available energy for the process which is applied to the heating of the component at the interface through frictional contact has been estimated. Thus, the available energy left to produce the mechanical deformation via the flash formation can be calculated by subtracting the thermal energy from the total energy. This is of importance to the manufacturing engineer. A method of validating the FE modelling predictions was proposed using high-speed photography methods during the process to understand the rotational speed of the moving part at the instant that the steady-state deformation commences. Results from FE modelling and experiment suggest that the width of the steady-state thermal profile formed through the IFW, and the time taken to reach steady-state is strongly dependent upon the applied pressure parameter.

Keywords: Mechanics, Kinetic, Thermal, Ti-6Al-4V, Equilibrium, Steady-state, Analytical

1. Introduction

Rotary friction welding is an advanced joining process, whereby two components with axial symmetry at the weld joint can be bonded using heat generated solely from the frictional interface caused by relative motion between the two^[1]. A so-called Inertia friction weld (IFW) is a type of rotary friction weld process, whereby kinetic energy stored in a rotating flywheel is converted into

frictional thermal energy to mostly join two components of cylindrical geometry. One component is clamped to the rotating flywheel, whilst the other component is clamped in a non-rotating tooling, connected to a hydraulic ram^[1]. During welding, the flywheel is brought to a certain rotation speed and a forging pressure is applied to the hydraulic ram to bring the two components to contact. The flywheel rotational velocity starts to decelerate owing to the conservation of the stored energy into thermal energy, causing the temperature to increase sharply at the interface owing to the generated friction^[1]. The relative motion at the interface allows for a heating and plasticisation of the interfacial material, and large deformations – characterised by the distinctive flash formation associated with a rotary friction weld. Friction welding processes, typically the IFW process considered in this work and linear friction welding, are often described as consisting of a number of different “stages” or “phases” of the process. The conditioning phase is defined as the initial phase whereby heat is generated from solid friction between one stationary and one moving part^[2]. During the conditioning phase no bulk deformation is observed, simply the flattening of surface asperities. Following the conditioning phase, the equilibrium phase sees weld line material extruded as flash, as a thermal equilibrium is achieved^[2].

The process of IFW differs from the more commonly used Direct-drive rotary friction welding (DDRFW) simply in the mechanics of delivering the kinetic energy to the one side of the rotating component as it is joined with a stationary counterpart. Whilst the commonly used DDRFW process uses an electric motor to drive the rotating part at a constant rotational velocity, the IFW process uses a flywheel. This produces a velocity that is not constant during processing, but continually decreasing until the flywheel has used up all of the stored kinetic energy. In manufacturing terms, the DDRFW process is limited as electric motors with the capability to run at such high speeds and deliver the torque required would need to be huge. Realistically, only very small components can be joined with even modern DDRFW machines. Whereas, IFW machines on the other hand simply need a large flywheel which can be wound to store the required kinetic energy to join sizeable metallic parts through friction processing.

However, during an IFW process, the kinetic energy delivered from the flywheel, must be converted partially to heat (through frictional contact and material shear) and partially to mechanical deformation to form the axial shortening and extruded material (flash) formation. The amount of kinetic energy needed to be provided to the flywheel to produce a certain amount of mechanical deformation is therefore difficult to ascertain. A model to help predict the amount of energy that is consumed through thermal loading is of great use to the manufacturing engineer. Energy balance calculations can prove a useful method of determining how much energy has gone in to heating of a part, and therefore how much is left for the mechanical deformation of the part. Appealing to basic physical relationships, it is feasible to calculate how much energy is consumed to produce the steady-state thermal cycles present in the material at the onset of mechanical deformation. An understanding

of how the various IFW process parameters influence the energy used to heat the part to its steady-state thermal cycle can then be drawn.

Finite element (FE) modelling of the IFW process has been studied and performed for a number of years, dating as far back as the 1990's^[3-5]. Some of the more successful models^[6-9] have conventionally considered the problem using a 2 ½ D modelling environment, whereby the model considers a cross section of the axi-symmetric problem, but also calculates the out-of-plane rotational velocity associated with the component. Previous FE models of the IFW process have generally considered the friction welding of steels^[6] and of nickel superalloys^[7-9] reflecting the common materials attached using this joining technology. Some models also considered the joining of two different materials (dissimilar welding)^[5-6]. However, the technology is rapidly being considered and developed for a wider range of materials, including the common titanium alloy Ti-6Al-4V, which is frequently used within the aerospace industry. As a result, FE models are also being advanced and developed to consider the IFW processing of such materials^[10].

2. Methodology

Experimental IFW joints using small testpiece specimens have been carried out at a selection of the process parameters considered here (see Table 1). The variations in the axial shortening caused by the mechanical deformation at the weld line is evidenced (Fig. 1), thus the energy supplied by the flywheel to the testpiece, which in turn gets converted in to mechanical work, must vary. It therefore becomes of great importance to be able to calculate the quantities of the total supplied flywheel energy required to; a) form the thermal profile present throughout welding, and b) leave a sensible amount of remaining energy available for mechanical work.

The presence of a steady-state thermal condition within a friction weld has been established within literature previously^[11]. The steady-state condition applies to the “equilibrium” phase, when the generation of heat inputted in to the system by friction and shear methods balances out the heat leaving the weld joint in to the flash. If an assumption is made that the IFW joint reaches its thermal steady-state condition as the onset of mechanical deformation begins (mechanical deformation being the process of axial shortening and flash forming), then we can equate the energy used by the conditioning phase with the energy used to form the steady-state thermal profile. The fundamental principles of rotational motion apply to the case of a rotary friction welded component. If we assume that the inertia of the combined system of flywheel and rotating workpiece remains constant throughout the process (ie: the flywheel is considerably more massive than the workpiece, thus the deformation of the workpiece will have a negligible effect upon the inertia of the overall system), then

it is possible to express the kinetic energy available from the stored potential energy within the system as:

$$E_{rot} = \frac{1}{2} \phi I \omega^2 \quad \dots\dots\dots(\text{Equation 1})$$

And the angular momentum of the system is defined as:

$$L_{rot} = \phi I \omega \quad \dots\dots\dots(\text{Equation 2})$$

Where I is the system rotational inertial mass, ω is rotational velocity and ϕ is a frictional loss term. Now, assume that during the initial stages of a rotary friction weld the available energy must be used in the heating of the weld interface volume, and the deformation only commences once a satisfactory thermal profile has been established at the interface. Therefore it is possible to calculate exactly how much of the total energy is consumed by the development of a thermal profile across the weld interface. By assuming the thermal profile is 1-dimensional (in the z -axis – see Fig 2), and therefore is uniform across the r and θ axes, it is possible to compute the energy required to heat the workpiece by considering the specific heat equation for materials:

$$\Delta Q = m \cdot c_p \cdot \Delta T \quad \dots\dots\dots(\text{Equation 3})$$

Whereby in the experimental set-up for the case of a friction weld, the increase in temperature ΔT is a function of the axial height $T(z)$, and where specific heat c_p is a function of Temperature, thus $c_p(T\{z\})$. Therefore, the chain rule is used to determine:

$$dQ = m \cdot c_p(z) \cdot \frac{dT}{dz} dz \quad \dots\dots\dots(\text{Equation 4})$$

And by taking the integral of both side of Equation 4, a simplistic 1D analytic model is obtained:

$$Q = \int m \cdot c_p(z) \frac{dT}{dz} dz \approx m \cdot \sum_j c_p(z_j) \frac{dT}{dz_j} | \forall x_j \quad \dots\dots\dots(\text{Equation 5})$$

Whereby the mass, m can be calculated using $m = \rho V$ (where ρ is density (assumed constant) and V is volume). By approximating the heated material to be represented by thin “strips” of material, whereby the delta T across the strip was relatively small, thus a constant c_p value could be assumed to represent the material specific heat capacity over the strip, so it is possible to estimate the energy taken to achieve the heating in the un-deformed workpiece to reach the steady-state thermal profile, at the instant that mechanical deformation is about to begin. Due to FE modelling mesh requirements and the Deform v11.0 software automatically re-meshing many times during the IFW model due to severe deformation, some pragmatism on strip width selection was required. Thus the various strip widths for different models were allowed to vary by a small amount, based upon nodal positions.

In order to perform this analytic calculation, an understanding of the thermal gradients at the weld interface and across the heated material, at the onset of mechanical deformation, is required. The most accurate methodology of obtaining this would be to take a series of thermal measurements from different distances away from the weld interface, to build up an understanding of the heating during the conditioning phase of a rotary friction weld. This could potentially be performed with a thermocouple-instrumented weld specimen. However, more practically, a FE model of the 2D weld cross section could be constructed, and thermal profiles extracted from this FE model, at the instant that mechanical deformation (in the form of upsetting) is about to commence. Previous work in the literature has utilised FE to solely consider the thermal loading during a friction weld, including the impacts of the process parameters^[12]. The FE model developed here has been demonstrated to offer a robust and reasonably accurate modelling method when considering the critical mechanical outputs from a rotary friction weld, including mechanical deformation and rotational speeds^[10].

Using the FE model, it is possible to split the workpiece up into thin “strips” the width of the elements in the z-axis, and calculate the energy required to raise material to match this thermal profile, from an initial room temperature state. This does of course assume that a “mean” temperature from each strip is considered, and also assumes that the c_p value across the strip of material is constant.

A finite element modelling methodology (see Fig. 2) representing an IFW of hollow cylinders has been based upon the 2½ D axi-symmetric methodology developed in literature^[6-7] with a torsional 2D element-type. Using the general purpose FE software package Deform (v11.0), representative 2½ D models of the two workpieces (illustrating the wall cross-section) and machine tooling have been developed. The model considers a visco-plastic element formulation in the two workpieces, thus will neglect the elastic strains that are experienced within the specimen during the process. Given the large deformations experienced, this is considered a reasonable assumption, given that the process is dominated by the plastic strain terms.

In reality, the IFW process will be supplied energy by both the flywheel tooling and the forging tooling. However, the energy contribution from the forging tooling is very small in size in comparison to the energy contribution from the flywheel, and as such is ignored for simplicity. Boundary conditions to represent thermal and mechanical constraints at the interfaces have been set-up. A flywheel / process efficiency of 1.0 was assumed. A biased mesh has been created, with finer elements of ~0.25mm at the weld line, coarsening to ~3½ mm away from the weld line. Given the considerable deformation experienced by the weld line region to form the flash material, the FE software had to be set to automatically re-mesh based upon certain mesh quality criteria. An element interference depth parameter was used, as recommended by the software suppliers^[14].

A frictional relationship, expressed as a function of temperature has been developed, to replicate the friction experienced at this interface. The relationship acts at the nodal point of each element at the workpiece – workpiece interface. The frictional law was empirically devised to best replicate the required thermal field, and is of the format expressed in Equation 6, where T is the nodal point temperature. For temperatures between roughly 1100 °C and 1250 °C, which is reported ^[7,8,16] typically to be the weld line temperature experienced, the frictional relationship must yield an appropriate coefficient, using a and b values which are material dependent and to be determined. Note that the frictional coefficient is described as a function of temperature, which in turn is highly dependent upon the processing parameters of rotational velocity and pressure.

$$f = a \ln(T) - b \quad \text{Where } 100\text{ }^{\circ}\text{C} < T < 1400\text{ }^{\circ}\text{C} \quad \dots \text{Equation (6)}$$

A material model for Ti-6Al-4V has been defined, based upon thermo-physical data commonly available within commercial software ^[13]. Stress-strain curves, defined to be dependent upon temperature and strain rate, have been developed from a combination of sources within the literature^[13], and through project industrial sponsorship, to produce a material model which best replicates the behaviour of this commonly used titanium alloy, within the extreme physical process of IFW.

3. Results

A series of FE models using the modelling set-up as described, have been built, considering a variety of welding parameters, as defined in Table 1a. As can be seen from the process parameter matrix, weld models 1-5 form a sensitivity study for the input Pressure parameter, with all other parameters remaining constant. Similarly, weld models 1 and models 6-9 form a sensitivity study for the Initial rotational speed parameter, with all other parameters remaining constant.

The FE models were simulated, and at the instance of flash formation beginning to occur, a 1D thermal profile was extracted from each model, as used as the thermal field for the analytic methodology.

Weld No.	Inertia, I (kgm^2)	Init. rotation speed, ω (rad/s)	Pressure, P (MPa)	Tot. kinetic Energy, $E_{\text{rot}} = 0.5I\omega^2$ (J)	Angular momentum, $L_{\text{rot}} = I\omega$ ($\text{kgm}^2\text{s}^{-1}$)
1	18.6	185	100	318,292 ½	3441
2	18.6	185	40	318,292 ½	3441
3	18.6	185	80	318,292 ½	3441
4	18.6	185	120	318,292 ½	3441

5	18.6	185	150	318,292 ½	3441
6	18.6	160	100	238,080	2970
7	18.6	135	100	169,492 ½	2511
8	18.6	115	100	122,992 ½	2139
9	18.6	100	100	93,000	1860

Table 1a: Weld parameters used for the series of nine FE models set-up.

Outputted thermal profiles from the 9 finite element models are shown in Fig. 3 (models 1-5 varying the applied pressure) and in Fig. 4 (models 1 and 6-9 – varying the initial rotational speed). Using the proposed analytic model, and assuming an efficiency factor of 1.0, the total energy available to the component for welding can be calculated for each weld. Recall the assumption that at the onset of mechanical deformation, the workpiece has reached an approximate steady-state thermal profile. Note that the applied axial pressure is predicted to have no impact on the total rotational energy available. However, it will clearly have an impact regarding the rate at which the energy is dissipated, as the applied pressure across the interface acts as the braking mechanism for the rotational velocity. Clearly, the energy required to form the thermal profile at the onset of mechanical deformation can only be a proportion of the total energy supplied by the rotating flywheel. It therefore becomes of interest to understand what proportion of the total available energy is being consumed by the heating of the specimen to form the thermal profile, and what energy therefore is left-over to mechanically deform the weld sample. Based upon the calculations performed using the 9 Finite element models, the energy consumed to form the steady-state thermal profile has been calculated.

Weld No.	Total kinetic Energy $E_{rot} = 0.5I\omega^2$ (J)	FE / analytic predicted energy to form thermal profile (J)	FE / analytic predicted rot. speed remaining (rad/s)	Measured* energy to form thermal profile (J)	Measured* Rot. speed remaining (rad/s)	Numerical modelling error** (%)
1	318,292½	94,090	155.3	106,805	150.8	-11.9
2	318,292½	174,490	124.3	194,872	115.2	-10.5
3	318,292½	103,306	152.0	124,106	144.5	-16.8
4	318,292½	79,950	160.1	88,765	157.1	-9.9
5	318,292½	81,013	159.7	Experiment not performed		
6	238,080	90,777	125.9	119,118	113.1	-23.8
7	169,492½	99,796	86.6	116,621	75.4	-14.4
8	122,992½	104,132	45.0	Experiment not performed		
9	93,000	98,432	0	Experiment not performed		

*Table 1b: Experimental validation of FE model to predict energy consumed to form thermal profile during conditioning. *Note: Measurements are estimated from high-speed photography images. **the modelling error calculated is of the predicted energy taken to form thermal profile.*

4. Experimental Validation of FE modelling

Any FE modelling activity requires a rigorous experimental procedure to demonstrate modelling accuracies and errors. Validation of this FE model to predict energy consumption during the different phases of the IFW process is difficult, given how challenging it would be to make accurate calculations regarding the energy remaining mid-way through a process that could not be halted. However, a method was considered to use high-speed photography to make approximations regarding the rotational speed at the instant that flash formation and upsetting commences (thus representing the end of the conditioning phase of the IFW process).

High-speed photography methods can be awkward to implement given the requirement for a line-of-sight to the specimen, the requirements for excess lighting of the specimen given the rapid shutter speed of the camera and the analysis of the data once a process has been recorded. For this experiment, a Photron FastCAM Mini UX100 was employed. Due to the required window of view and the length of time to record for (typically 3-5 seconds), a frame rate of 10,000 fps was used. One non-intrusive marking was added to the visible region of the rotating workpiece to provide a datum point to estimate rotational speed from the video.

The outputted video files were studied to observe the moment at which the bulk deformation and flash formation commenced, to indicate the end of the conditioning phase and the commencement of the steady-state phase of the IFW process. Some pragmatism must be adopted to rationalise the instant that the conditioning phase finishes. The rotational speed at the onset of steady-state flash formation was approximated based upon the time taken to complete the final full rotation, indicated by non-intrusive surface marks on the specimen, before bulk flash formation commenced.

Validation experiments suggest that the numerical modelling developed to estimate the energy consumed in the conditioning phase (forming the thermal profile) is slightly under-predicting the energy taken to perform the conditioning phase, thus over-predicting the true remaining rotational speed (see Table 1b). Under-prediction of energy taken to perform the conditioning phase at the relevant time-frame was typically between 9-16% for the welds varying the applied pressure, although were as high as 24% for the welds with very low initial rotational speed.

This under-prediction in the rotational speed remaining (and hence over-prediction of the energy taken to complete the conditioning phase) in the FE model is likely caused by small variations in the

heat capacity across each strip within the FE model, where the analytical method considered here is assuming this is constant. Additionally, the analytical model is assuming that up to the instance of flash formation there is zero mechanical work done. In reality, the IFW specimen will inevitably display some small degree of deformation, thereby this energy need to cause the small deformations during the conditioning phase is not considered.

5. Discussion

From Table 2, there appears a clear trend in the results from weld models 1-5 that as the applied pressure increases, the width of the steady-state thermal profile at the onset of deformation reduces, and as such, so does the energy consumed to form this thermal profile (see Fig. 5). As a greater axial pressure is applied across the weld, so the layer of heated material is forced out in to the extruded flash material faster, leaving behind a narrower layer of material heated through frictional and shearing effects at the interface. The steady-state thermal profile is formed when the heat influx at the weld interface due to frictional and shear effects balances the removal of heat through flash removal and through the thermal conductivity and heat transfer mechanisms within the Ti-6Al-4V part itself.

Whereas, Fig. 6 suggests that the initial rotational speed only acts as a very minor influence upon the formed thermal profile at steady-state, when deformation commences, compared to the influence of pressure. Note that the result from weld 9 is discounted as it is not thought to have achieved steady-state yet. However, it is evident from Fig. 6 that the peak weld line temperature of the 100rad/s weld in particular was so low (1015°C) because this weld did not offer enough energy in total to form the steady-state welding thermal profile. This is also understood to be the reason why the 115rad/s weld predicts slightly lower peak weld line temperatures (1200°C), although in the case of this weld, it does carry on after the steady-state profile is formed, to give a small amount of upset.

Weld No.	Total Energy available (J)		Calculated energy for thermal profile (J)	Remaining energy for mechanical work (J)	% of energy used in thermal formation	Time taken to reach steady-state (s)
1	318,292½		94,090	224,192½	29.6%	0.91
2	318,292½		174,490	143,792½	54.8%	2.12
3	318,292 ½		103,306	214,976½	32.4%	0.99
4	318,292½		79,950	238,332½	25.1%	0.78
5	318,292½		81,013	237,269½	25.5%	0.69
6	238,080		90,777	147,303	38.1%	1.05
7	169,492½		99,796	69,696½	58.9%	1.16
8	122,992½		104,132	18,660½	84.7%	1.33

9	93,000		98,432	-5, 432	105.8%	Not reached...
----------	--------	--	--------	----------------	--------	----------------

Table 2: Results of the finite element weld models, including energy consumed by the forming of the thermal profile, and the time taken to reach the thermal profile.

It would be beneficial to further understand the influence of these two process parameters. Considering the impacts that the applied pressure has initially, it is observed that the increase in energy required to form the thermal profile as pressures decreases is clearly not a linear trend. Indeed it appears to form an approximate $y = \frac{1}{x}$ type curve (see Fig. 7a). The physical meaning of this relationship between the applied pressure parameter and the thermal profile requires some further consideration. A $y = \frac{1}{x}$ type relationship would imply that as pressure decreases, so the thermal profile widens. Given that higher pressures introduce more energy in to the system, this initially appears counter-intuitive. However, recall that the contribution of energy to the system from the forging tooling is considered small in comparison to the energy contribution from the flywheel, so this additional energy added becomes negligible. Now, by considering increasing the pressure for fixed flywheel energy (as per welds 1-5), so a greater pressure will force the highly viscous hot layer of material out of the joint and in to the flash at a faster rate, thus leaving a narrower thermal profile within the joint. This is highly analogous to the process of linear friction welding, which yields a narrower thermal profile for higher pressure welds ^[15].

Taking weld model 1 (100MPa applied pressure) as a baseline, the difference in energies required to form the steady-state thermal profile for the maximum attempted pressure of 150MPa (an increase in applied pressure of 50MPa) is relatively small (13kJ less, ~14% reduction), whereby the difference in energies required for the lowest pressure weld attempted (a reduction in applied pressure of 60MPa) is huge (80kJ more, ~85% increase). This does suggest that the majority of pressures tested within this sensitivity study are forming a similar steady-state thermal profile (as evidenced in Fig. 5), whereas the very lowest pressure weld model is much further across on this $y = \frac{1}{x}$ curve, and as such it has taken considerably more energy to form the thicker steady-state profile.

Now considering the initial rotational speed parameter, it is clearly observed that this parameter has considerably less influence over the shape of the thermal profile formed, and as such the energy consumed in forming the thermal profile (Fig. 7b). This trend could possibly be considered linear. Potentially it might be argued that the selected sensitivity study hasn't explored the lower region of the design space at all, however by considering the results from weld 9, it can be observed that all of the available energy from the flywheel has been consumed in forming a thermal profile, and continuing the argument from previously that weld 9 appears to have not yet reached a steady-state

thermal profile, the experiment has found the lower bound for the successful IFW application in this titanium alloy. It is therefore possible to calculate the minimum required energy to simply produce a bonded joint occurs at approximately the 115rad/s, 18.6kgm² flywheel condition, which in turn yields a total energy of 122,992.5 J. This would suggest that there is required a minimum available amount of energy left after forming the steady-state thermal profile to allow for some mechanical deformation, to consider the bond successfully formed. By the matrix considered here, this minimum energy available for mechanical deformation would be the remaining energy left after forming steady-state in weld 8, ~18-20kJ.

If the weld is therefore considered to be formed after this relatively small quantity of energy is consumed through mechanical deformation, then this would suggest that a successful bond was formed between the two components very early on in to the mechanical deformation stage for a lot of the welds considered here. By considering the baseline weld 1 model, this had an available 224kJ for mechanical deformation after forming the steady-state thermal profile. Assuming that only 18-20kJ is required in mechanical deformation to form a bond, it becomes evident that the successful bond was formed well before the end of the mechanical deformation stage of the process.

In order to reason why the weld model 9 appears to have produced a thermal profile containing a fraction more heat energy than the total energy available from the flywheel, it is important to consider the original assumptions. The assumption of a simplistic 1-dimensional thermal profile has been considered within the analytic model. However, there will be some variation from this simplistic thermal profile across the width of the sample. Additionally, recall that an assumption made that the energy introduced in to the process was supplied entirely by the flywheel. In reality, a small amount of additional energy is supplied by the forging tooling, however this has been considered negligible in comparison. As the amount of flywheel energy reduces, so the contributions of energy from the forging tooling becomes more significant, and could introduce some small errors in to the numerical analysis.

The time taken to reach the steady-state thermal profile has been computed from the FE models (see Fig. 8). There appear to be very similar trends in the time taken to reach steady state as there is for the energy used, for both process parameters, again close to a $\frac{1}{x}$ relationship for the pressure and a linear relationship for the rotational speed.

6. Conclusions

A 2½ D finite element model has been built, which has allowed for greater understanding of the energies associated with the formation of a steady-state thermal profile during the initial stages of

Inertia friction welding (IFW). An assumption is made that the steady-state thermal profile across the weld interface is formed by the onset of mechanical deformation (axial shortening and flash formation), and that thermal profile is 1-dimensional. This thermal profile is then fed in to an analytical model to estimate the energy consumed by the formation of the thermal profile. The FE / analytical model approach has been validated using experimental welds and high-speed photography. The following conclusions are drawn from this work:

- The steady-state thermal profile formed appears strongly dependent upon the applied pressure process parameter, although appears to be weakly-dependent of the initial rotational speed parameter (assuming enough energy is supplied by the flywheel). As pressure decreases, so the width of the steady-state thermal profile increases, to follow a $\frac{1}{x}$ type relationship, where x is the applied pressure parameter.
- A weld which has a very low energy input may not attain its steady-state thermal profile before the total available energy is entirely dissipated. In which case, no deformation (flash formation) will be observed. Further, it is suggested that a minimum of 18-20kJ energy is required to be consumed in mechanical deformation before a successful weld interface bond is formed.
- The time taken to reach steady-state thermal profile follows a similar $\frac{1}{x}$ relationship with axial pressure that was observed for the energy consumed in forming the thermal profile.

Acknowledgements

The authors wish to thank the European Regional Development fund (ERDF) for financial support of this work, as a part of the CASiM² project, a collaborative research project considering modelling and simulation methods between the University of Birmingham, Rolls-Royce plc and the MTC. Thanks are offered to Dr Steve Beech and Ben Saunders (Rolls-Royce plc), Dr Hannah Edmonds (MTC) and Dr Joao Gandra (TWI) for their assistance with the work.

References

1. Attallah MM, Preuss M, *Welding and Joining of Aerospace Materials*, Woodhead Publishing, 25-74 (2012).
2. Vairis A., Frost M., High frequency linear friction welding of a titanium alloy, *WEAR*, 217;1, 117-131 (1998).
3. Moal A, Massoni E , Chenot JL, A finite element model for the simulation of the torsion and torsion-tension tests *Comp. Methds App. Mech & Eng.*, 103:3, 417-434 (1993).

4. Moal A, Massoni E, Finite element simulation of the inertia welding of two similar parts *Engineering Computations*, 12:6, 497-512 (1995).
5. D'Alvise L, Massoni E, Walloe S, Finite element modelling of the inertia friction welding process between dissimilar materials *J. Mat. Proc. Tech.*, 125-6, 387-91 (2002).
6. Bennett C, *PhD thesis – University of Nottingham* (2006).
7. Bennett C, Attallah M, Preuss M, Shipway P, Bray S. Finite element modelling of the inertia friction welding of dissimilar high strength steels, *MMTA*, 44, 11, 5054-64 (2013).
8. Grant B, Preuss M, Withers P, Rowson M, Finite element process modelling of inertia friction welding advanced nickel-based superalloy, *Mat Sci Eng A*. 513-4, 366-75 (2009).
9. Wang F, Li W-Y, Li J-L, Vairis A, Process parameter analysis of inertia friction welding nickel-based superalloy, *Int J Adv. Manuf Tech*, 71:1, 1909-1918 (2014).
10. Turner R, Howe D, Thota B, Basoalto HC, Brooks JW, Modelling & Validation of the Inertia Welding Process for Ti-6Al-4V, *OPTIMoM conference* , Oxford (2014).
11. Turner R, Ward RM, Gebelin J-C, Reed RC, Linear Friction Welding of Ti-6Al-4V: modelling and Validation, *Acta Mater.*, 59:10, 3792-3803 (2011).
12. Cheng L, Li W-Y, Li J-L, *J. Shanghai Jiatong Univ. (Sci.)*, 16: 3, 277-280 (2011).
13. JMatPro - Sente Software Ltd, 40 Occam Rd, Surrey Technology Centre, Guildford, UK.
14. Scientific Forming Technologies Corp. (SFTC), 2545 Farmers Drive, Columbus, Ohio 43235, USA.
15. R. Turner, EngD Thesis, University of Birmingham (2010).
16. L. Yang, PhD Thesis, University of Birmingham (2010).

Vitae

Dr Richard Turner is a Research Fellow in the School of Metallurgy & Materials, at the University of Birmingham. His areas of research are friction weld processes and the numerical simulation of these.

Mr Dan Howe is a Computational Engineer in Materials and Process Modelling at Rolls-Royce plc. Dan has worked on numerical simulation projects, including frictional processing, for a number of years.

Mr Bhaskar Thota is now a Business Development manager at the MTC Ltd, although at the time of research was a Research Fellow in the School of Metallurgy & Materials, at the University of Birmingham.

Dr Mark Ward is a Senior Lecturer in the School of Metallurgy and Materials, University of Birmingham, working at improving materials and processes by applying mathematical modelling, electrical and electronic engineering and more general sensing and control techniques.

Dr Hector Basoalto is a Senior Research Fellow and Technical director of the Partnership for Research in Simulation of Manufacturing and Materials (PRISM²) at the University of Birmingham.

His research explores the causal relationships between microstructure, deformation and mechanical properties of engineering alloys using multi-scale modelling techniques.

Professor Jeffery Brooks is the Director of the Partnership for Research in Simulation of Manufacturing and Materials (PRISM²) at the University of Birmingham. He has developed FE modelling techniques for stress analysis and manufacturing process simulation, and is developing methods to apply these within an integrated computational materials engineering (ICME) framework.

Tables

Weld No.	Inertia, I (kgm ²)	Init. rotation speed, ω (rad/s)	Pressure, P (MPa)	Tot. kinetic Energy, $E_{\text{rot}} = 0.5I\omega^2$ (J)	Angular momentum, $L_{\text{rot}} = I\omega$ (kgm ² s ⁻¹)
1	18.6	185	100	318,292 ½	3441
2	18.6	185	40	318,292 ½	3441
3	18.6	185	80	318,292 ½	3441
4	18.6	185	120	318,292 ½	3441
5	18.6	185	150	318,292 ½	3441
6	18.6	160	100	238,080	2970
7	18.6	135	100	169,492 ½	2511
8	18.6	115	100	122,992 ½	2139
9	18.6	100	100	93,000	1860

Table 1a: Weld parameters used for the series of nine FE models set-up.

Weld No.	Total kinetic Energy $E_{\text{rot}} = 0.5I\omega^2$ (J)	FE / analytic predicted energy to form thermal profile (J)	FE / analytic predicted rot. speed remaining (rad/s)	Measured* energy to form thermal profile (J)	Measured* Rot. speed remaining (rad/s)	Numerical modelling error** (%)
1	318,292½	94,090	155.3	106,805	150.8	-11.9
2	318,292½	174,490	124.3	194,872	115.2	-10.5
3	318,292½	103,306	152.0	124,106	144.5	-16.8
4	318,292½	79,950	160.1	88,765	157.1	-9.9
5	318,292½	81,013	159.7	Experiment not performed		
6	238,080	90,777	125.9	119,118	113.1	-23.8
7	169,492½	99,796	86.6	116,621	75.4	-14.4

8	122,992½		104,132	45.0		Experiment not performed
9	93,000		98,432	0		Experiment not performed

*Table 1b: Experimental validation of FE model to predict energy consumed to form thermal profile during conditioning. *Note: Measurements are estimated from high-speed photography images.**the modelling error calculated is of the predicted energy taken to form thermal profile.*

Weld No.	Total Energy available (J)		Calculated energy for thermal profile (J)	Remaining energy for mechanical work (J)	% of energy used in thermal formation	Time taken to reach steady-state (s)
1	318,292½		94,090	224,192½	29.6%	0.91
2	318,292½		174,490	143,792½	54.8%	2.12
3	318,292 ½		103,306	214,976½	32.4%	0.99
4	318,292½		79,950	238,332½	25.1%	0.78
5	318,292½		81,013	237,269½	25.5%	0.69
6	238,080		90,777	147,303	38.1%	1.05
7	169,492½		99,796	69,696½	58.9%	1.16
8	122,992½		104,132	18,660½	84.7%	1.33
9	93,000		98,432	-5, 432	105.8%	Not reached...

Table 2: Results of the finite element weld models, including energy consumed by the forming of the thermal profile, and the time taken to reach the thermal profile.

Figures

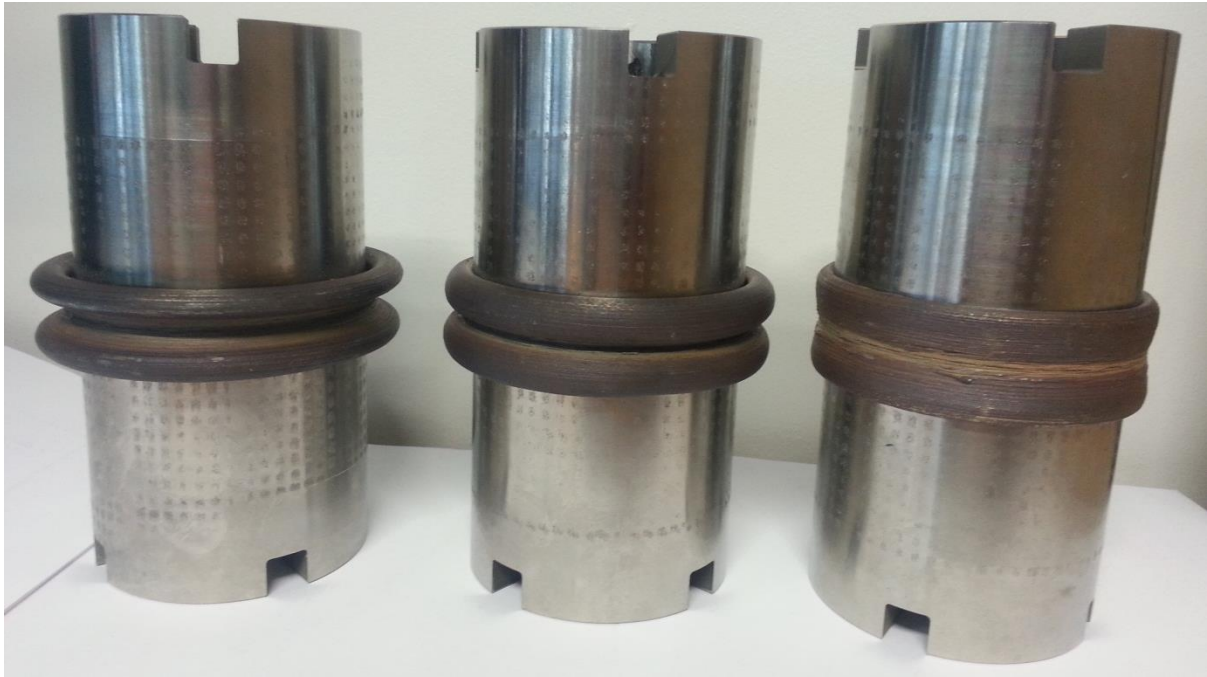


Figure 1: Examples of 3 IFW Ti-6Al-4V specimens at varying process parameters within the considered matrix.

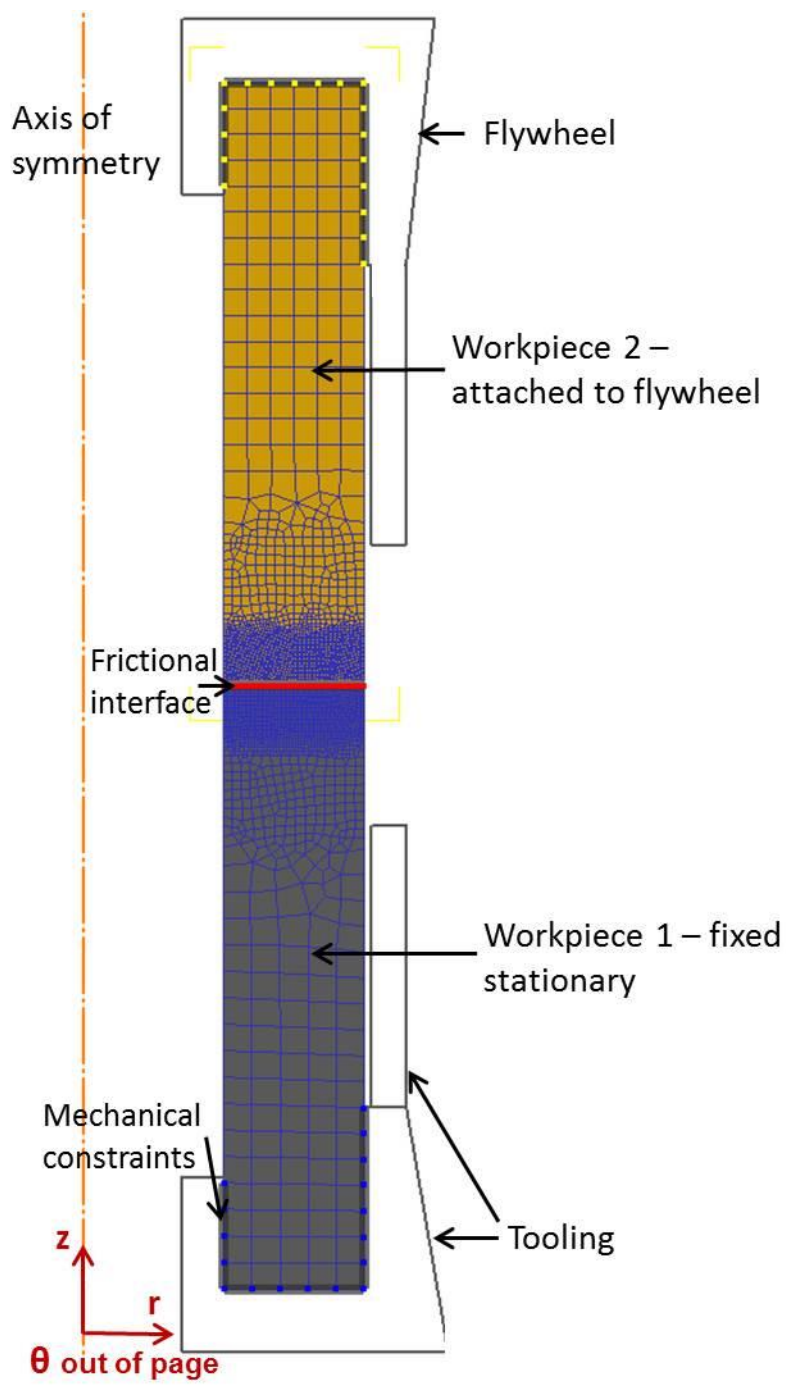


Figure 2: Set-up of the IFW model in the FE software Deform (v11.0)

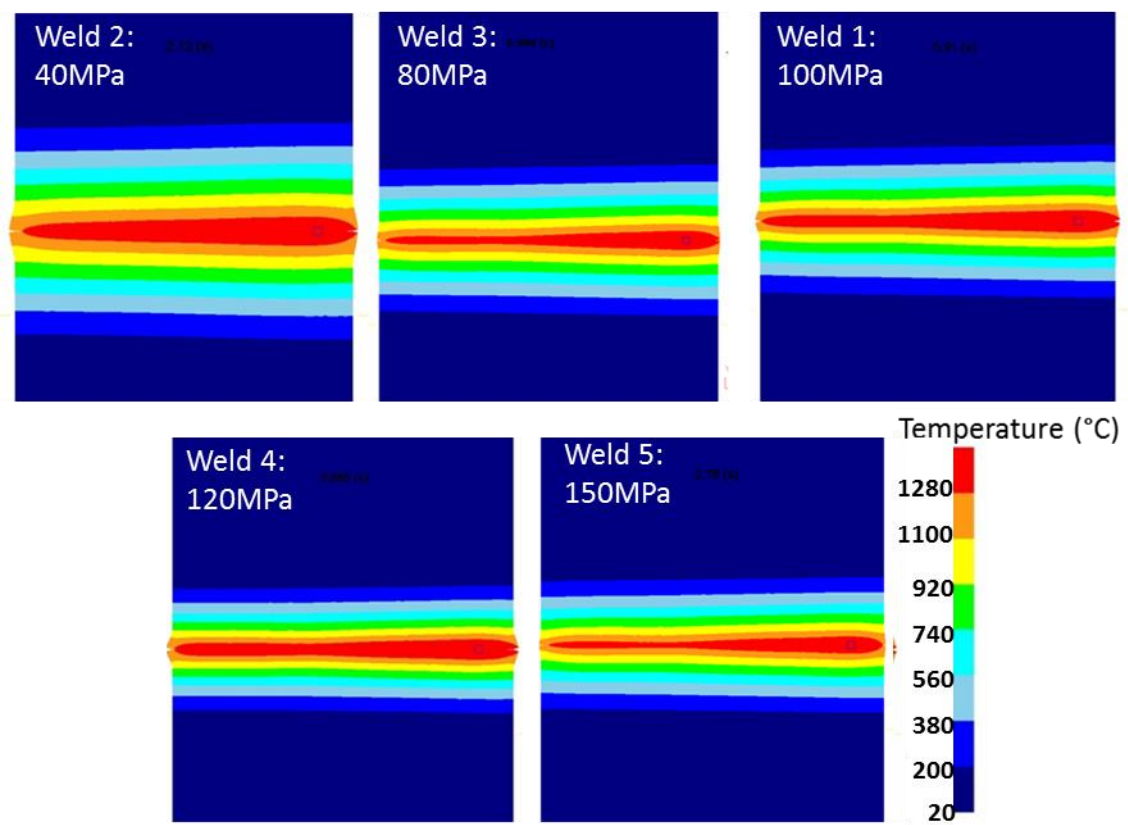


Figure 3: Thermal profiles from weld models 1-5 for varying applied pressure.

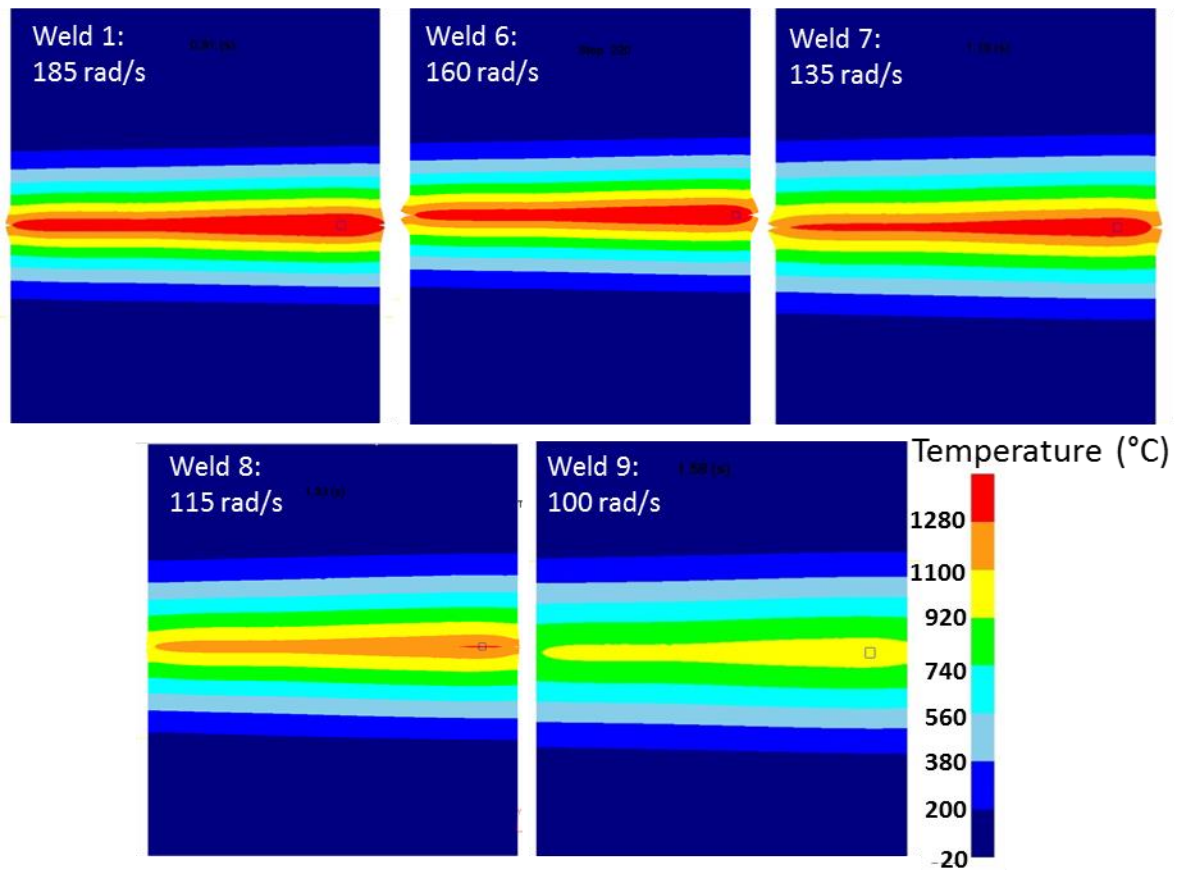


Figure 4: Thermal profiles from weld models 1 & 6-9 for varying initial rotational velocity.

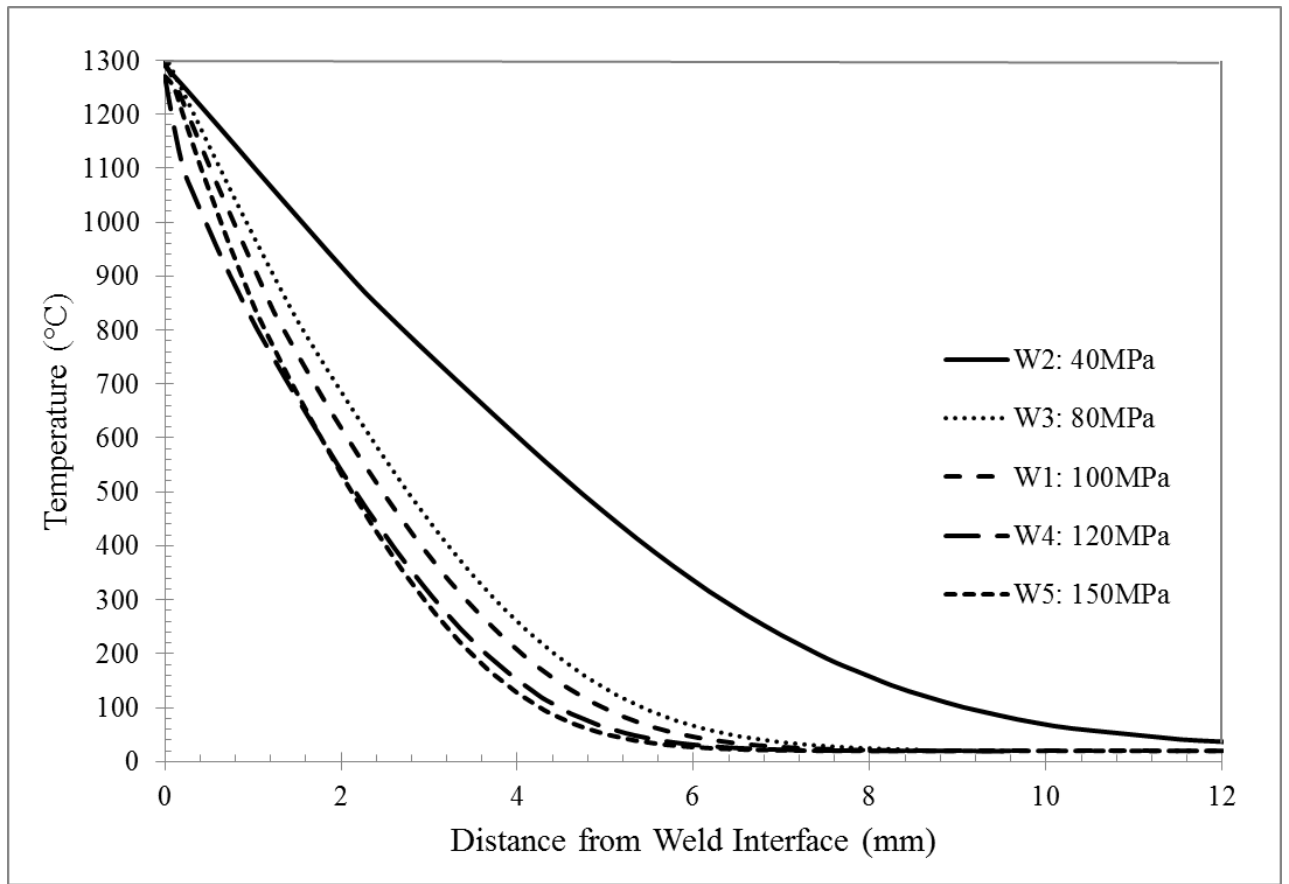


Figure 5: Steady-state thermal profiles from models 1-5, varying applied pressure, 40MPa, 80MPa, 100MPa, 120MPa and 150MPa.

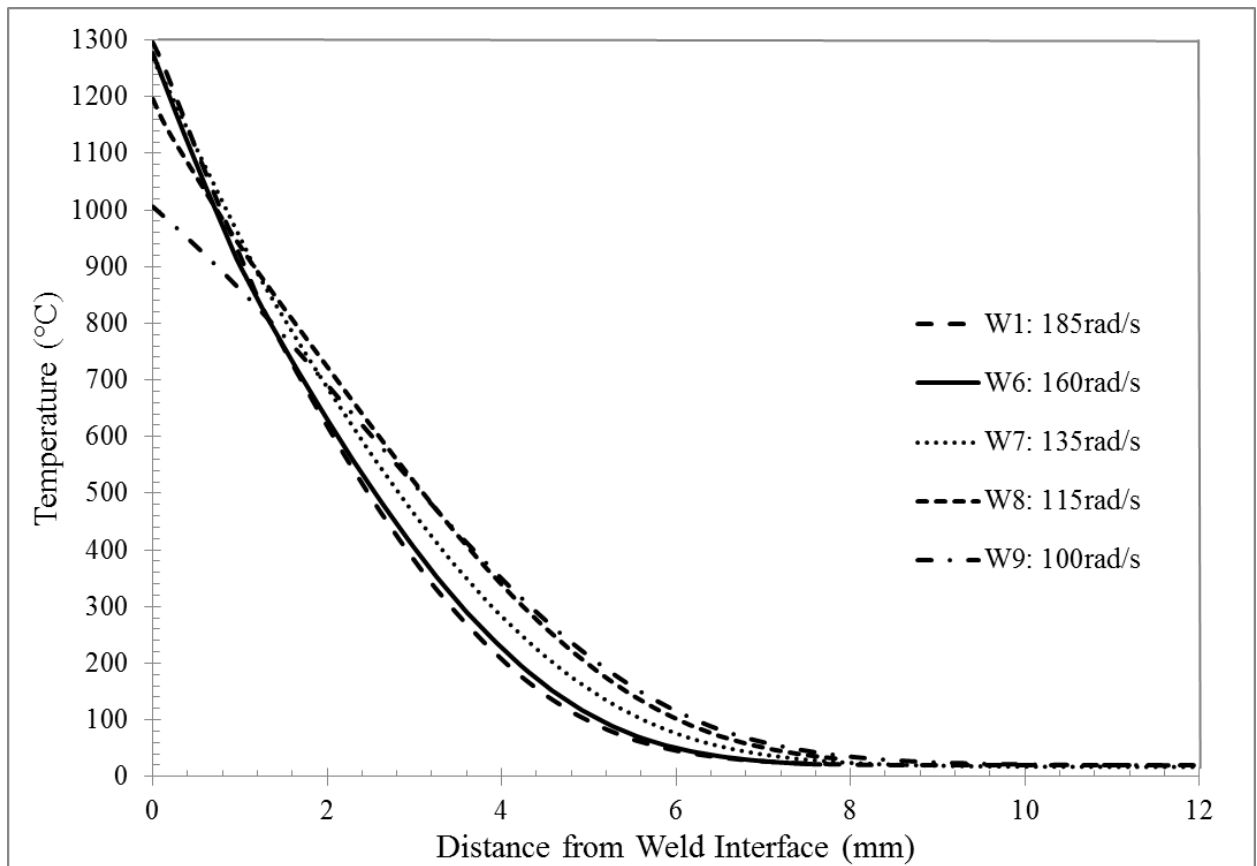


Figure 6: Steady-state thermal profiles from models 1 & 6-9, varying the initial rotational speed, 100rad/s, 115rad/s, 135rad/s, 160rad/s and 185rad/s.

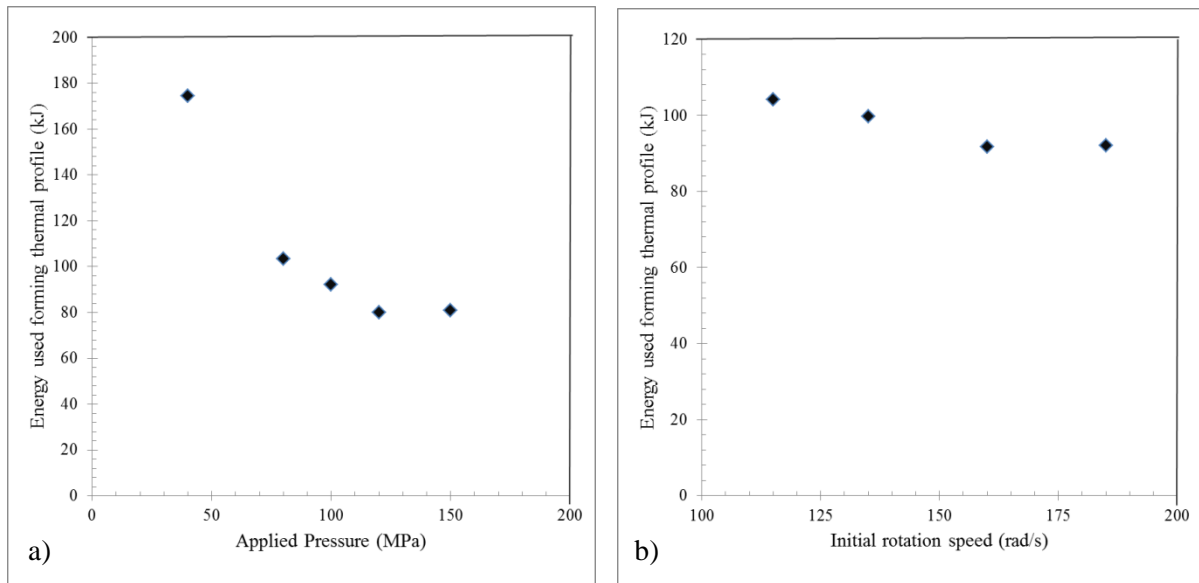


Figure 7: Graph illustrating energy used during the formation of the thermal profile as a function of (a) the applied pressure parameter, and (b) the initial rotation speed (Note: Weld model 9 wasn't included as it was felt that this had not attained its steady-state profile before all total energy available was exhausted).

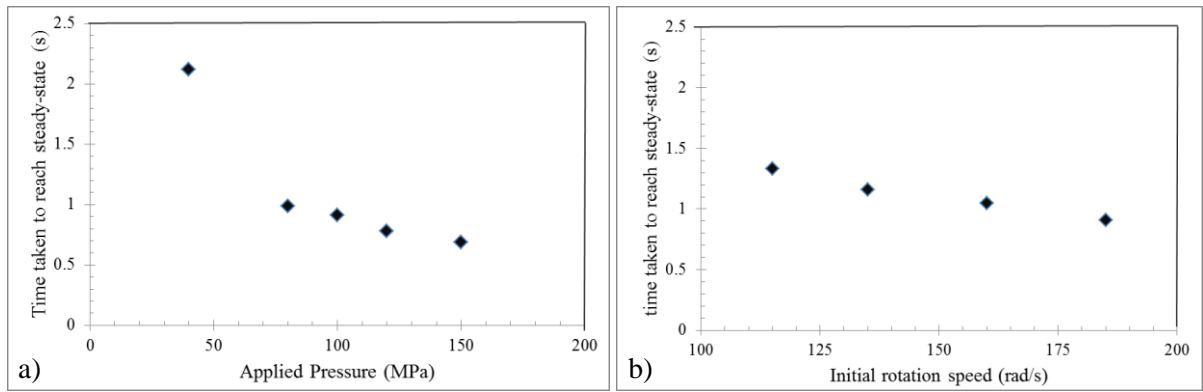


Figure 8: Graph illustrating time taken to reach steady-state thermal profile as a function of (a) the applied pressure parameter, and (b) the initial rotation speed (Note: weld model 9 not included as it did not reach steady-state).